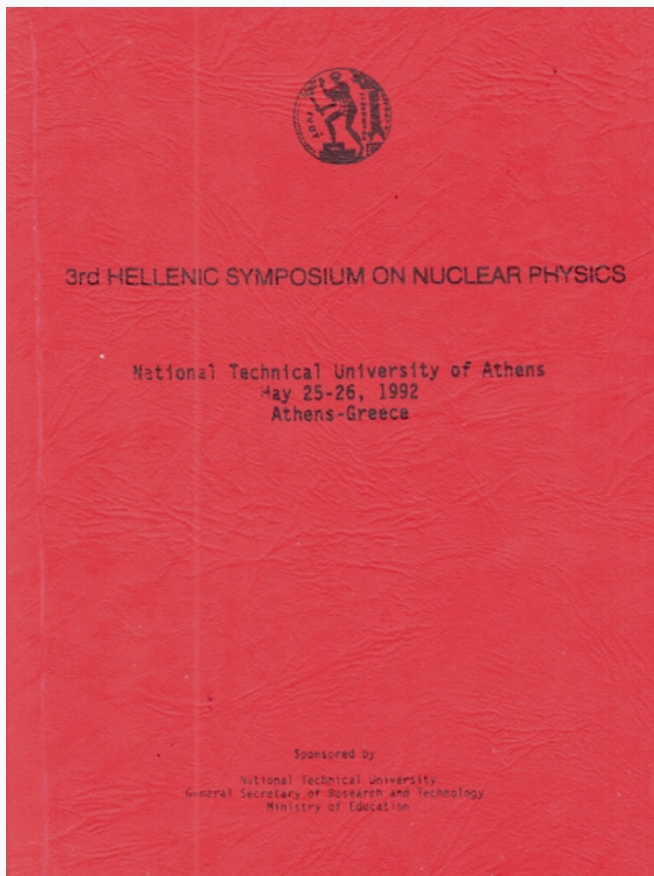


## HNPS Advances in Nuclear Physics

Vol 3 (1992)

HNPS1992



**Root mean square radii of the  $\Lambda$ -particle orbits in hypernuclei using potentials of orthogonal shape in arelativistic treatment**

*C. G. Koutroulos, G. J. Papadopoulos*

doi: [10.12681/hnps.2362](https://doi.org/10.12681/hnps.2362)

### To cite this article:

Koutroulos, C. G., & Papadopoulos, G. J. (2019). Root mean square radii of the  $\Lambda$ -particle orbits in hypernuclei using potentials of orthogonal shape in arelativistic treatment. *HNPS Advances in Nuclear Physics*, 3, 20–38. <https://doi.org/10.12681/hnps.2362>

Root mean square radii of the  $\Lambda$ -particle orbits in  
hypernuclei using potentials of orthogonal shape in  
a relativistic treatment

C.G.Koutroulos and G.J.Papadopoulos

Department of Theoretical Physics

Aristotle University of Thessaloniki

54006 Thessaloniki, Greece

Abstract

The root mean square radii of the  $\Lambda$ -particle orbits in hypernuclei are calculated in the ground and first excited states using the Dirac equation with scalar and vector potentials of orthogonal shape. An exact analytic and also approximate expressions are derived for the root mean square radius of the  $\Lambda$  orbit in its ground state. It is shown that  $\langle r^2 \rangle_{s_{1/2}}^{1/2}$  varies linearly with  $A_{\text{core}}^{1/3}$  for the higher mass hypernuclei. Our results in the ground state are compared with the results of Rayet and also with those of Daskaloyannis et. al.

## 1. Introduction

The radii of the orbits which the  $\Lambda$ -particle can occupy inside the  $\Lambda$ -hypernuclei is a subject which attracted the interest of several authors in the past. Though there are no experimental results with respect to which one can compare his theoretical results, yet the problem is interesting. In some previous publications we have considered this subject using the Woods-Saxon potential and also the potential  $U(r) = -D/\cosh^2(r/R)$ . These results were obtained entirely by numerical calculations.

In this paper we consider the same problem assuming that the  $\Lambda$ -nucleus potential is made up of an attractive  $U_s(r)$  and a repulsive  $U_v(r)$  components both of orthogonal shape and that the equation of motion of the  $\Lambda$ -particle in hypernuclei is the Dirac equation.

The reason behind this choice of potential is not because one expects an improvement of the results already obtained using the more realistic Woods-Saxon potential but because in the square well case one obtains analytic solutions for the wavefunctions in all bound states. (Note that the square well potential belongs to the few cases for which the Dirac equation is solvable analytically.) Using the wavefunctions the root mean square radii of the orbits of the  $\Lambda$ -particle in hypernuclei can be calculated either numerically or analytically in terms of the potential parameters. We mention also that in the square well case one can derive an eigenvalue equation holding for all the states from which the binding energies  $B_\Lambda$  of the  $\Lambda$ -particle in hypernuclei can be calculated.

In section 2 of this paper the basic formalism used in our calculations is explained, while in section 3 our results are given and discussed.

## 2. Formalism

We assume that the potential between the  $\Lambda$ -particle and the nucleus is made up of an attractive component  $U_s(r)$  and a repulsive component  $U_v(r)$ . We assume also that the differential equation describing the motion of the  $\Lambda$ -particle in hyper-  
(7-10)  
nuclei is the Dirac equation

$$(c\vec{\alpha} \cdot \vec{p} + \beta\mu c^2 + \beta U_s(r) + U_v(r))\psi = E\psi \quad (1)$$

where  $\vec{\alpha} = (\alpha_1, \alpha_2, \alpha_3)$ ,  $\beta$  are the Dirac matrices.  $E$  is the total energy i.e.  $E = -B_\Lambda + \mu c^2$ ,  $B_\Lambda$  being the binding energy of the  $\Lambda$  particle.  $\psi$  is the Dirac four-spinor which may be written as

$$\psi = \psi_{nljm} = \begin{pmatrix} iG_{nlj}(r)(1/r) \\ F_{nlj}(r)\vec{\sigma} \cdot \vec{r}(1/r) \end{pmatrix} \phi_{ljm} \quad (2)$$

Instead of the potentials  $U_s(r)$  and  $U_v(r)$ , the potentials

$$U_{\pm}(r) = U_s(r) \pm U_v(r) \quad (3)$$

are used, which are both attractive.

From the Dirac equation (1) one obtains by the procedure outlined in refs (7-10) the following radial differential equation of the Schrödinger type

$$g''(r) - \left\{ \frac{l(l+1)}{r^2} + \frac{2\mu}{\hbar^2} (V_{\text{centr.}}(r, B_\Lambda) + V_{\text{s.o.}}(r, B_\Lambda) + B_\Lambda) \right\} g(r) = 0 \quad (4)$$

where  $V_{\text{centr.}}(r, B_\Lambda)$  is the central part of the potential and  $V_{\text{s.o.}}(r, B_\Lambda)$  the spin orbit part of it. The complete expressions of these potentials are given in ref. (10).

The solution  $g(r)$  of the differential equation (4) is related to the large radial component  $G(r)$  of the Dirac wavefunction through the formula

$$G(r) = D^{1/2}(r)g(r) \quad (5)$$

where

$$D(r) = \frac{1}{\hbar c} \{ 2\mu c^2 - B_\Lambda + U_-(r) \}. \quad (6)$$

The small radial component of the Dirac wavefunction is related to  $G(r)$  by means of the formula

$$F(r) = (G'(r) + \frac{\kappa}{r}G(r))D^{-1}(r) \quad (7)$$

(where we have suppressed the quantum numbers  $n, l, j$  in  $G(r)$  and  $F(r)$ ) and  $\kappa = \pm(j + (1/2))$  for  $j = l \pm (1/2)$ .

Assuming that the potentials  $U_+(r)$  and  $U_-(r)$  are square wells with depths  $D_+$  and  $D_-$  and the same radius  $R$  i.e.

$$U_\pm(r) = -D_\pm (1 \pm \theta(r-R)) \quad (8)$$

where  $\theta$  is the unit step function and  $R = r_0 A_{\text{core}}^{1/3}$ , the corresponding differential equation can be solved analytically for all bound states as it was pointed out in ref (12). The wavefunctions  $G(r)$  and  $F(r)$  are given by the following expressions

$$G(r) = N \left\{ (1 - \theta(r-R)) j_1(\eta r) r + \theta(r-R) \frac{j_1(\eta R)}{h_1^{(1)}(\eta_0 R)} h_1^{(1)}(\eta_0 r) r \right\} \quad (9)$$

$$\begin{aligned}
 F(r) = Nc\hbar \{ & (1-\theta(r-R)) \frac{1}{(2\mu c^2 - B_\Lambda - D_-)} \left( r \frac{dj_1(\eta r)}{dr} + (\kappa + 1) j_1(\eta r) \right) \\
 & + \theta(r-R) \frac{1}{(-B_\Lambda + 2\mu c^2)} \frac{j_1(\eta R)}{h_1^{(1)}(i\eta_0 R)} \left( r \frac{dh_1^{(1)}(i\eta_0 r)}{dr} \right. \\
 & \left. + (\kappa + 1) h_1^{(1)}(i\eta_0 r) \right) \} \quad (10)
 \end{aligned}$$

where

$$\eta = \left\{ \frac{2\mu}{\hbar^2} (D_+ - B_\Lambda) (1 - (B_\Lambda + D_-) (2\mu c^2)^{-1}) \right\}^{1/2} \quad (11)$$

$$\eta_0 = \left\{ \frac{2\mu}{\hbar^2} B_\Lambda (1 - B_\Lambda (2\mu c^2)^{-1}) \right\}^{1/2} \quad (12)$$

and  $j_1(\eta r)$  ;  $h_1^{(1)}(i\eta_0 r)$  are the spherical Bessel and Hankel functions of the first kind. The normalization constant N follows from the following normalization condition

$$\int_0^\infty (G^2(r) + F^2(r)) dr = 1 \quad (13)$$

With the help of the wavefunctions G(r) and F(r) we have calculated the root mean square radii of the  $\Lambda$  particle orbits in hypernuclei using the formula

$$\langle r^2 \rangle_{s1/2}^{1/2} = \left\{ \frac{\int_0^\infty r^2 (G^2(r) + F^2(r)) dr}{\int_0^\infty (G^2(r) + F^2(r)) dr} \right\}^{1/2} \quad (14)$$

For the ground state the above integrals were calculated analytically and the corresponding <sup>expression for the</sup> root mean square radius is

$$\langle r^2 \rangle_{s1/2}^{1/2} = N_0 \left\{ \frac{R^3}{6} - \frac{R^2 \sin(2\eta R)}{4\eta} - \frac{R \cos(2\eta R)}{4\eta^2} + \frac{\sin(2\eta R)}{8\eta^3} + \right.$$

$$\frac{c^2 \hbar^2}{(2\mu c^2 - B_{\Lambda} - D_-)^2} \left( \frac{\eta^2 R^3}{6} + \frac{\eta R^2 \sin(2\eta R)}{4} + \frac{R^2 \cos(2\eta R)}{4} - \frac{5 \sin(2\eta R)}{8\eta} + \frac{R}{2} + \frac{R \cos(2\eta R)}{2} \right) + \frac{\sin^2(\eta R) (2\eta_0^2 R^2 + 2\eta_0 R + 1)}{4\eta_0^3} + \frac{c^2 \hbar^2 \sin^2(\eta R)}{(-B_{\Lambda} + 2\mu c^2)^2} \frac{2\eta_0^2 R^2 + 4\eta_0 R + 5}{4\eta_0} \}^{1/2} \quad (15)$$

The normalization constant  $N_0$  is given by the expression

$$N_0 = \left\{ \frac{R}{2} - \frac{\sin(2\eta R)}{4\eta} + \frac{\sin^2(\eta R)}{2\eta_0} + \frac{c^2 \hbar^2 \sin^2(\eta R)}{(-B_{\Lambda} + 2\mu c^2)^2} \left( \frac{\eta_0}{2} + \frac{1}{R} \right) + \frac{c^2 \hbar^2}{(2\mu c^2 - B_{\Lambda} - D_-)^2} \left( \frac{\eta^2 R}{2} + \frac{\eta \sin(2\eta R)}{4} - \frac{\sin^2(2\eta R)}{2R} \right) \right\}^{-1/2} \quad (16)$$

The above analytic expression of the root mean square radius can be simplified further by ignoring the less significant terms. In this case we find the following expression

$$\langle r \rangle_{s_{1/2}}^{1/2} = \frac{R}{3^{1/2}} \left[ 1 - \frac{2 \left( \frac{\sin(2\eta R)}{2\eta R} - \frac{\sin^2(\eta R)}{\eta_0 R} \right) - 3 \left( \frac{\sin^2(\eta R)}{\eta_0^2 R^2} - \frac{\cos(2\eta R)}{2\eta^2 R^2} \right)}{1 - \left( \frac{\sin(2\eta R)}{2\eta R} - \frac{\sin^2(\eta R)}{\eta_0 R} \right)} \right]^{1/2} \quad (17)$$

which can be simplified further and leads to the expression

$$\begin{aligned} \langle r \rangle_{s_{1/2}}^{1/2} &= \frac{R}{3^{1/2}} - \frac{\sin(2\eta R)}{2\eta 3^{1/2}} + \frac{\sin^2(\eta R)}{\eta_0 3^{1/2}} \\ &= \frac{R}{3^{1/2}} + \frac{1}{2\eta_0 3^{1/2}} - \frac{\sin(2\eta R + \phi)}{2\eta_0 3^{1/2} \sin \phi} \end{aligned} \quad (18)$$

where  $\phi = \text{arccot}\left(\frac{\eta_0}{\eta}\right)$  .

Other similar approximate expressions were derived which are less accurate.

Expression (18) can be simplified further by observing that the ratio  $(\sin(2\eta R + \phi))/\sin\phi$  varies between the values -1.13 and -1.35 for almost the entire range of hypernuclei and it can be approximated by the intermediate value -1.2 holding for most of the higher mass hypernuclei in which case we find the expression

$$\langle r^2 \rangle_{s_{1/2}}^{1/2} = \frac{R}{3^{1/2}} + \frac{1.1}{\eta_0 3^{1/2}} = \frac{r_0}{3^{1/2}} A_{\text{core}}^{1/3} + \frac{1.1}{\eta_0 3^{1/2}} . \quad (19)$$

This expression is of the form  $c A_{\text{core}}^{1/3} + b$  (where  $c, b$  constants) i.e. it is linear in  $A_{\text{core}}^{1/3}$  for large  $A_{\text{core}}$ . A result of this form was shown to hold for the Woods-Saxon potential but it was derived using an entirely different argument. (4) Note that in (19)  $\eta_0$  is energy dependent. It can be replaced by the energy independent quantity

$$\eta_0(\text{ap}) = \left\{ \frac{2\mu}{\hbar^2} D_+ (1 - D_+ (2\mu c^2)^{-1}) \right\}^{1/2} \quad (20)$$

derived from  $\eta_0$  by taking  $B_{\Lambda} = D_+$  which is a rather good approximation for sufficiently heavy hypernuclei. Better approximate expressions may also be used. (10, 12, 13)

If in expression (18) instead of using the assumption  $(\sin(2\eta R + \phi))/\sin\phi = -1.2$  the trigonometric functions are expanded separately using the formula  $\sin x \approx x$  we find for  $\langle r^2 \rangle_{s_{1/2}}^{1/2}$  the following approximate expression



$$\langle r^2 \rangle_{S^{1/2}}^{1/2} \approx \frac{r_0}{3^{1/2}} \left\{ 1 - \left( \frac{D_+}{B_\Lambda} - 1 \right)^{1/2} \left( 1 - \frac{D_-}{4m_\Lambda c^2} \right) \right\} A_{\text{core}}^{1/3} +$$

$$\frac{\hbar c}{2(3^{1/2})(2m_\Lambda c^2)^{1/2}} \left\{ \frac{1 + \frac{3\pi}{2}}{B_\Lambda^{1/2}} + \frac{1 + \frac{D_-}{4m_\Lambda c^2}}{(D_+ - B_\Lambda)^{1/2}} \right\} \quad (21)$$

which is of the form  $cA_{\text{core}}^{1/3} + b$ , where  $c$  and  $b$  are (energy dependent) constants. In this expression additional terms involving negative powers can be included. The omitted part is the following:

$$+ \frac{r_0}{3^{1/2}} \frac{D_-}{4m_\Lambda c^2} \left( \frac{D_+}{B_\Lambda} - 1 \right)^{1/2} A_{\text{core}}^{-2/3} +$$

$$\frac{\hbar c}{2(3^{1/2})(2m_\Lambda c^2)^{1/2}} \left[ \frac{1 + \frac{3\pi}{2}}{2B_\Lambda^{1/2}} + (D_+ - B_\Lambda)^{-1/2} \left( \frac{3D_-}{8m_\Lambda c^2} + 0.5 \right) \right] A_{\text{core}}^{-1} +$$

$$\frac{\hbar c}{2(3^{1/2})(2m_\Lambda c^2)^{1/2}} (D_+ - B_\Lambda)^{-1/2} \frac{D_-}{8m_\Lambda c^2} A_{\text{core}}^{-2} + \dots$$

This part does not contribute significantly in the case of the higher mass hypernuclei while in the case of the small mass hypernuclei, for instance around  ${}^{13}_\Lambda\text{C}$  its contribution is 5%. From the first term of (21) one can see that the slope of the curve changes sign when  $B_\Lambda = 0.5(1 - D_-(4m_\Lambda c^2)^{-1})D_+ = 14$  MeV which is true for hypernuclei between  ${}^{16}_\Lambda\text{O}$  and  ${}^{28}_\Lambda\text{Si}$  (see fig.1).

Finally in the ground state the  $\langle r^2 \rangle_{s_{1/2}}^{1/2}$  can be calculated approximately from the formula

$$\hbar\omega_{\Lambda} \approx \frac{3}{2} \frac{\hbar^2}{\mu} \frac{1}{\langle r^2 \rangle_{s_{1/2}}} \approx \Delta_{sp} \quad (22)$$

where  $\Delta_{sp} = B_{\Lambda}(1s) - B_{\Lambda}(1p)$ . Of course it is understood that this formula is not relativistic (like for instance (15)) despite of the fact that the binding energies involved in it were obtained relativistically. It can merely be used to give a first estimate of the root mean square radii.

### 3. Numerical results and comments.

Numerical calculations of the root mean square radii of the  $\Lambda$ -particle orbits in its ground and excited states in hypernuclei were performed using the definition (expression (14)) and the results obtained with potential parameters  $r_0 = 1.01$  fm,  $D_+ = 30.55$  MeV and  $D_- = 300$  MeV are shown in table 1.

In table 2 the root mean square radii of the  $\Lambda$ -particle orbits in its ground state in hypernuclei are given; calculated using a) the analytic expression (15) see col.II and b) the approximate expressions (17) see col.III, (18) see col.IV, (19) see col.V, (21) see col.VI, (22) see col.VII, In col. VIII the results obtained using in expression (19) instead of  $\eta_0$  the quantity  $\eta_0(\text{ap})$  derived from  $\eta_0$  by replacing  $B_\Lambda$  by  $D_+$ , are given. The potential parameters used in obtaining the results of this table are the same as those used in table 1.

In table 3 the root mean square radii of the  $\Lambda$ -particle orbits in hypernuclei in the states  $1s_{1/2}$ ,  $1p_{3/2}$ ,  $1p_{1/2}$  obtained using the square well potential with the same parameters as those of table 1 are compared / the corresponding results obtained using the Woods-Saxon potential with parameters  $a = 0.6$  fm,  $r_0 = 1.198$  fm,  $D_+ = 29.8$  MeV and  $D_- = 300$  MeV. (Note that the extra decimals given in our results are given for the sake of comparison.)

In figure 1 the results given in table 1 i.e. the  $\langle r_\Lambda^2 \rangle^{1/2}$  in the states  $1s_{1/2}$ ,  $1p_{3/2}$ ,  $1p_{1/2}$ ,  $1d_{5/2}$ ,  $1d_{3/2}$ ,  $1f_{7/2}$ ,  $1f_{5/2}$  are plotted versus  $A_{\text{core}}^{1/3}$ . The corresponding points are indicated by shaded triangles ( $\blacktriangle$ ). In the same table also our results concerning the ground state obtained using the Woods-Saxon potential with the parameters of table 3 are plotted. The corresponding points are indicated by shaded dots ( $\bullet$ ). For comparison we give also for the ground state the results of Rayet indicated by squares ( $\blacksquare$ ) and the results of Daskaloyannis

et. al. indicated by crosses (X) which in both cases were obtained by a nonrelativistic approach.

Comparing the results of tables 1 and 2 we see that the results obtained numerically and analytically concerning the ground state are in a very good agreement..

..Comparing the results of table 2 obtained using the various approximate expressions we see that almost all of them are in good agreement among themselves and with the analytic one, except expressions (22) and (19) with  $B_{\Lambda}=D_{+}$  in the case of small  $A_{\text{core}}$ . In particular the error percentages observed in comparing the various approximate expressions with the analytic expression (15) are respectively for exp.(17) 0%-5%, for exp. (18) 6%-8%, for exp. (19) 5%-6% and for exp.(21) 0%-11%. Expression(19) is the most interesting because it shows immediately the two interesting features of the curve  $\langle r^2 \rangle_{s_1/2}^{1/2}$  versus  $A_{\text{core}}^{1/3}$ , i.e. first the linear behaviour of the curve for the large  $A_{\text{core}}$  which is deduced by setting  $B_{\Lambda}=D_{+}$  (see col.VIII of table 2) and secondly the deviation from linearity for the small  $A_{\text{core}}$  which is deduced from the fact that the second term in (19) depends inversly on  $\eta_0$  which is energy dependent and so for small binding energies (i.e. for small  $A_{\text{core}}$ ) the curve rises above the straight line obtained for  $B_{\Lambda}=D_{+}$ . To be more precise the rising above the straight line is observed through out the entire range of the  $\Lambda$ -hypernuclei but is small for the hypernuclei with large  $A_{\text{core}}$  and so the straight line forms a good approximation of the curve as far as down to  ${}_{\Lambda}^{28}\text{Si}$  (see fig. 1. Also compare columns V and VIII of table 2). Expression (22) is

referred here because it gives an alternative way of a rough estimate of  $\langle r^2 \rangle_{s^{1/2}}^{1/2}$ . Its degree of accuracy can be immediately viewed from table 2.

Comparing the results of tables 2 and 3 (see also fig.1) we observe that the results obtained with the more realistic Woods-Saxon potential are a little different from those obtained with the square well potential, the difference being of the order of 7%-14% in the ground state. This is of course what one

should expect since for the Woods-Saxon potential  $r_0 = 1.198$  fm while for the square well potential  $r_0 = 1.01$  fm. As we see from formula (19) a larger value of  $r_0$  in the case of the square well potential would have increased the root mean square radius so as to make the difference with the Woods-Saxon potential minimum.

From fig. 1 we see that the root mean square radius shows a rather linear behavior with respect to  $A_{\text{core}}^{1/3}$  for the larger values of  $A_{\text{core}}$  not only in the ground state but also in the excited states. Graphically we find for the ground state that the equation of the straight line part of the curve is

$$\langle r^2 \rangle_{s^{1/2}}^{1/2} = c A_{\text{core}}^{1/3} + b = 0.5 A_{\text{core}}^{1/3} + 0.75$$

If the approximate formula (19) is used we find for

$$c = \frac{r_0}{3^{1/2}} \approx 0.58$$

and for

$$b = \frac{1.1}{\eta_0(\text{ap}) 3^{1/2}} \approx 0.48$$

Finally from fig. 1 we observe that our results in the ground state are slightly higher than the results of Rayet

and in a very good agreement with the results of Daskaloyannis et. al. obtained for a nonrelativistic square well potential with parameters  $r_0=1.035$  fm and  $D=29.5$  MeV.

#### Acknowledgments

We would like to thank Professor M.Grypeos for suggesting this investigation and for comments on the manuscript.

#### References

1. Rayet M 1976 Ann.Phys. 102 ,226
2. Daskaloyannis C B , Grypeos M E , Koutroulos C G , Massen S E and Saloupis D S 1984 Phys.Lett.134B ,147
3. Daskaloyannis C B , Grypeos M E , Koutroulos C G Massen S E and Saloupis D S 1983 Proceedings of the International Conference on Nuclear Physics Vol. 1, C87,405
4. Koutroulos C G 1990 Z.Naturforsch. 45a ,191
5. Koutroulos C G 1991 J.Phys.G:Nucl. Part. Phys. 17, 1069
6. Lalazissis G A, Grypeos M E and Massen S E 1988 Phys.Rev. C37, 2098
7. Brockmann R and Weise W 1977 Phys.Lett. 69B, 167
8. Brockmann R 1978 Phys.Rev. C18, 1510
9. Brockmann R and Weise W 1981 Nucl. Phys. A 355 , 365
10. Koutroulos C G and Grypeos M E 1989 Phys.Rev. C 40, 275
11. Koutroulos C G 1989 J.Phys.G:Nucl. Part. Phys. 15, 1659
12. Papadopoulos G J, Koutroulos C G and Grypeos M E 1991

2nd Hellenic Symposium on Nuclear Physics 389. (Submitted for publication)

13. Grypeos M E and Koutroulos C G 1986 Nucl.Phys A450, 307.

(Also work in progress)

14. Koutroulos C G 1990 First Hellenic Symposium on Theoretical Nuclear Physics 193

Table 1

Root mean square radii of of the  $\Lambda$ -particle orbits in the ground and excited states for various hypernuclei obtained numerically using the definition (expression (14)). The potential parameters used are  $r_0=1.01$  fm,  $D_+=30.55$  MeV,  $D_-=300$  MeV.

$A_{core}$	$\langle r^2 \rangle_{s_{1/2}}$ fm	$\langle r^2 \rangle_{p_{3/2}}$ fm	$\langle r^2 \rangle_{p_{1/2}}$ fm	$\langle r^2 \rangle_{d_{5/2}}$ fm	$\langle r^2 \rangle_{d_{3/2}}$ fm	$\langle r^2 \rangle_{f_{7/2}}$ fm	$\langle r^2 \rangle_{f_{5/2}}$ fm
8	2.11						
10	2.05						
11	2.05						
12	2.05						
15	2.07						
27	2.24						
31	2.30	2.89	2.88				
39	2.41	2.94	2.91				
50	2.54	3.05	3.01	3.75			
88	2.92	3.43	3.39	3.84	3.79		
137	3.27	3.84	3.78	4.22	4.15	4.55	4.51
207	3.69	4.27	4.24	4.67	4.61	4.99	4.91



Table 2

Root mean square radii of the A-particle orbits in the ground state for various hypernuclei obtained using the exact analytic expression (15) col.II and the approximate expressions (17) col.III, (18) col.IV, (19) col.V, (21) col.VI, (22) col.VII, (19) with  $B_A=D_+$  col.VIII.The potential parameters used are the same as those of table 1.

	Analytic exp. (15)	exp. (17)	exp. (18)	exp. (19)	exp. (21)	exp. (22)	exp. (19) with $B_A=D_+$
Acore	$\langle r^2 \rangle_{s_{1/2}}$ fm	$\langle r^2 \rangle_{s_{1/2}}$ fm	$\langle r^2 \rangle_{s_{1/2}}$ fm	$\langle r^2 \rangle_{s_{1/2}}$ fm	$\langle r^2 \rangle_{s_{1/2}}$ fm	$\langle r^2 \rangle_{s_{1/2}}$ fm	$\langle r^2 \rangle_{s_{1/2}}$ fm
8	2.11	2.00	2.17	2.21	2.04	-	1.68
10	2.05	1.99	2.15	2.16	2.03	-	1.77
11	2.05	2.00	2.15	2.16	2.04	-	1.81
12	2.05	2.01	2.16	2.17	2.05	-	1.84
15	2.07	2.06	2.20	2.20	2.10	-	1.94
27	2.25	2.26	2.41	2.40	2.34	2.11	2.24
31	2.31	2.32	2.46	2.46	2.42	2.16	2.32
39	2.42	2.44	2.60	2.59	2.56	2.26	2.47
50	2.55	2.58	2.75	2.74	2.72	2.39	2.64
88	2.93	2.96	3.17	3.15	3.19	2.70	3.08
137	3.28	3.31	3.55	3.54	3.63	3.10	3.50
207	3.70	3.73	4.01	3.97	4.12	3.46	3.93

Table 3

Comparison between the root mean square radii of the orbits of the  $\Lambda$ -particle in various hypernuclei obtained with the square well potential with parameters  $r_0=1.01$  fm,  $D_+=30.55$  MeV,  $D_-=300$  MeV and with the Woods-Saxon potential with parameters  $r_0=1.198$  fm,  $D_+=29.8$  MeV,  $D_-=300$  MeV,  $a=0.6$  fm in the states  $s_{1/2}, P_{3/2}, P_{1/2}$ .

Hyper-nuclei	Square Well			Woods-Saxon			
	$\langle r^2 \rangle_{s_{1/2}}$ , fm	$\langle r^2 \rangle_{P_{3/2}}$ , fm	$\langle r^2 \rangle_{P_{1/2}}$ , fm	$\langle r^2 \rangle_{s_{1/2}}$ , fm	$\langle r^2 \rangle_{P_{3/2}}$ , fm	$\langle r^2 \rangle_{P_{1/2}}$ , fm	$\langle r^2 \rangle_{P_{1/2}}$ , fm
$^{13}_\Lambda C$	2.05			2.39			
$^{16}_\Lambda O$	2.07			2.40			
$^{28}_\Lambda Si$	2.24			2.52			
$^{32}_\Lambda S$	2.30	2.89	2.88	2.54	3.32	3.32	3.32
$^{40}_\Lambda Ca$	2.41	2.94	2.91	2.67	3.37	3.35	3.35
$^{51}_\Lambda V$	2.54	3.05	3.01	2.79	3.47	3.45	3.45
$^{89}_\Lambda Y$	2.92	3.43	3.39	3.16	3.82	3.79	3.79
$^{138}_\Lambda B$	3.27	3.84	3.78	3.54	4.22	4.18	4.18
$^{208}_\Lambda Pb$	3.69	4.27	4.24	3.97	4.69	4.65	4.65

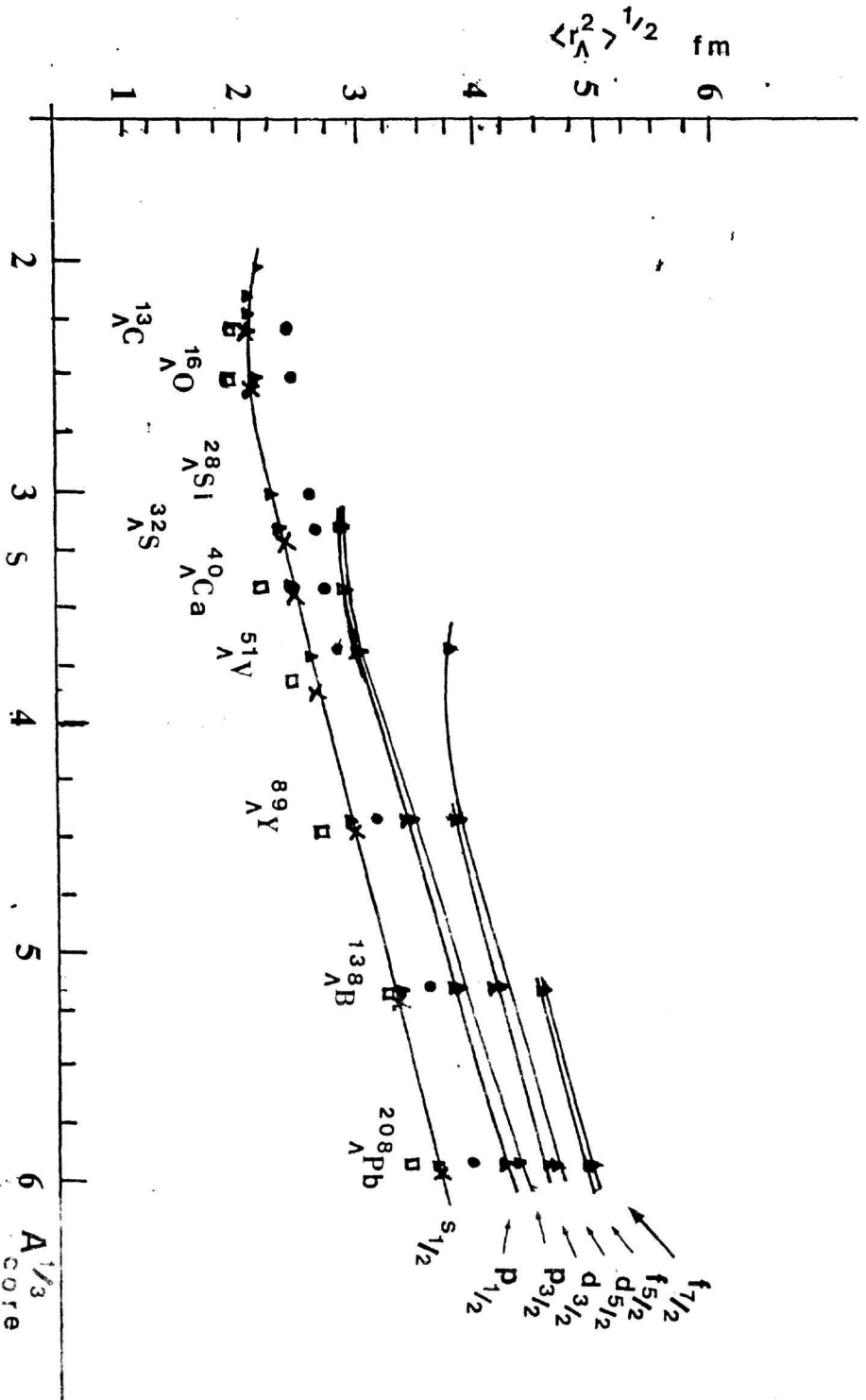


fig. 1

$A^{1/3}$   
core

Figure caption

Fig. 1: Variation of the  $\langle r_{\Lambda}^2 \rangle^{1/2}$  with  $A_{\text{core}}^{1/3}$  in the ground and first excited states of  $\Lambda$ -hypernuclei. Shaded triangles indicate the results obtained with orthogonal shape potentials while dots indicate the results (in the ground state) obtained with Woods-Saxon shape potentials. Empty squares indicate the results of Rayet and crosses the results of Daskaloyannis et. al. (both in the ground state).